Analysis of indirect measurement of cutting forces turning metal cylindrical shells

Kirill Kondratenko*[1], Alexandre Gouskov[1, 2], Mikhail Guskov[3], Philippe Lorong[3], Grigory Panovko[4]

1. Bauman Moscow State Technical University, Department RC5, Moscow, Russia.
2. National Research Centre "Kurtchatovsky Institute", Moscow, Russia.
3. ENSAM-ParisTech, Paris, France.
4. IMASH RSA, Moscow, Russia.

Email: kk92@ya.ru, gouskov_am@mail.ru, mikhail.guskov@ensam.eu, philippe.lorong@ensam.eu, gpanovko@yandex.ru.

Abstract Cutting forces measurement is an important component of the machining processes development and control. The use of conventional direct measurement systems is often impossible as they interfere in the process's dynamics. This work proposes a method of cutting force indirect estimation during turning thin-walled cylindrical shells. Calculation of the flexibility matrix has enabled us to relate measured displacements of certain workpiece's points to the cutting force. An optimization approach for choosing the measurement points location has been proposed, based on the best conditioning of the flexibility matrix.

Key words Cutting forces measurement, Thin-walled workpiece, Technological system, Optimization, Ill-conditioned systems.

1.0 Introduction

In modern manufacturing, cutting forces measurement is a key element in understanding the operational conditions during machining workpieces. Usually, cutting forces are measured directly using different kinds of dynamometers. For instance, in [1], an experimental set-up is described where cutting forces are measured directly, with a Kistler 9257B three-component piezo-dynamometer. The direct measurement approach is also incorporated in [2]. Another approach, based on the use of currents drawn by a.c. feed-drive servo motors, is presented in [3], where the pulsating milling forces are measured indirectly within the bandwidth of the current feedback control loop of the feed-drive system.

Nevertheless, in some cases, the use of dynamometers can be problematic, for instance in case of thin-walled workpieces in presence of instabilities: due to the presence of resonances in the frequency response of the dynamometer can induce

significant perturbations in the measured signals. This was the case for [4]: the addition of the dynamic system of the dynamometer has modified the conditions of the chatter onset.

In the present paper, we address the problem of quasi-static evaluation of the cutting force during turning cylindrical shells. The cutting force components are estimated indirectly, from the displacement measurements, with the help of the flexibility matrix, based on the elastic behavior of the structure.

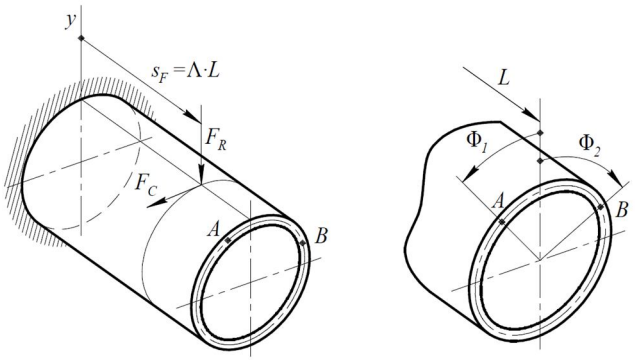

Fig. 1 The components of the cutting force (on the left). The free end of the shell (on the right) with angular location of the displacement sensors shown.

Two arbitrary points belonging to the free end of the shell are chosen: point A and B. The points represent the location of two displacement sensors. The angular location of these points is determined by parameters Φ_1 and Φ_2, which is shown in Fig. 1. The radial displacements of these points are actually measured using non-contact displacement sensors. The relation between the two components F_C, F_R of the cutting force and the radial displacements w_A and w_B of points A and B at first approximation is linear and injective:

$$\mathbf{A}\mathbf{f} = \mathbf{e} \tag{1}$$

where

$$\mathbf{A} = \begin{bmatrix} a_{11} & a_{12} \\ a_{21} & a_{22} \end{bmatrix}, \quad \mathbf{f} = \begin{bmatrix} F_C \\ F_R \end{bmatrix}, \quad \mathbf{e} = \begin{bmatrix} w_A \\ w_B \end{bmatrix}. \tag{2}$$

Matrix $\mathbf{A}$ is called the *flexibility matrix*. Parameter Λ determines the axial position of the cutting force. In order for the solution $\mathbf{f} = \mathbf{A}^{-1}\mathbf{e}$ to be reliable, system (1) has to be *numerically stable*. The system stays numerically stable as long as its condition number is sufficiently close to 1.The question of the optimality of the sensors position is sought in terms of the condition number of the flexibility matrix.

Section 2 addresses the algorithm of calculation of the flexibility matrix, and Section 3 describes a particular way of avoiding numerical instabilities calculating this matrix.

2.0 Calculation of the Flexibility Matrix

In this section, we develop a quasi-static analysis of the force-displacement relation applied to the case of turning a thin-walled cylindrical shell. The cutting force is taken as concentrated.

The shell is shown in Fig. 2. The left-hand edge of the shell is rigidly fixed, and the right-hand edge is free. In other words, the shell is supported like a cantilever with "clamped-free" boundary conditions. Thickness of the shell is regarded as being much smaller than its diameter: $h \ll D = 2R$. We will be using cylindrical coordinates: axial s and angular φ. An arbitrary point M belonging to the middle surface of the shell is said to have coordinates $(s,\ \varphi)$, as shown in Fig. 2.

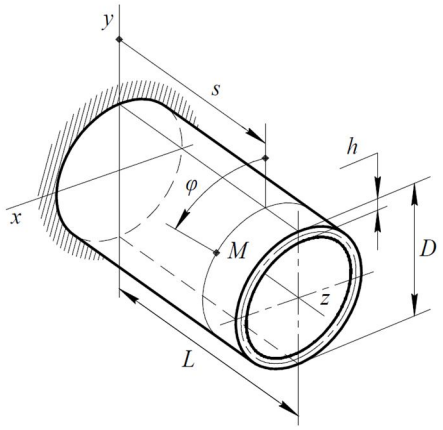

Fig. 2 The shell's dimensions and system of coordinates.

The shell is subjected to pin-load, which is represented by the two components of the cutting force: radial F_R and circumferential F_C, as shown in Fig. 1. We neglect the axial component of the cutting force because it is always much smaller than the other two components [4], and because the stiffness in the z-direction is much higher than in the other two directions. Forces F_C and F_R act on the point with coordinates $(s_F,\ 0)$. We introduce Λ as a changeable dimensionless parameter so that $s_F = \Lambda \cdot L$, see (Fig. 1). We can now write down the expression for the shell's thickness:

$$h(s) = \begin{cases} h_{\text{fin}} & \text{if } s < s_F \\ h_{\text{ini}} & \text{if } s \geq s_F \end{cases} \tag{3}$$

where h_{ini} is the shell's thickness before cutting and h_{fin} is the shell's thickness after cutting.

According to [6], the general system of equations for a Kirchhoff-Love thin-walled cylindrical shell shown in Fig. 2 may be written [10] in matrix form

$$\mathbf{L}\mathbf{y} = \mathbf{g} \tag{4}$$

where $\mathbf{L}$ is a linear partial differential operator represented by (8×8) matrix and

$$\mathbf{y} = \{u,\ v,\ w,\ \vartheta_1,\ RT_1,\ RS_1^*,\ RQ_1^*,\ RM_1\} \tag{5}$$

is the state vector and

$$\mathbf{g} = -R \cdot \{0,\ 0,\ 0,\ 0,\ q_1,\ q_2,\ q_3,\ 0\}. \tag{6}$$

is the load vector. Here R is the shell's radius, u is the axial direction displacement, v is the circumferential direction displacement, w is the radial direction displacement, ϑ_1 is the surface normal's angular displacement, T_1, S_1^*, Q_1^*, M_1 are the internal forces, and q_1, q_2, q_3 represent distributed external loading. Equation (4) represents a linear system of partial differential equations. It is possible to separate s and φ with the aid of the Fourier method using complex Fourier series:

$$\mathbf{y} = \sum_{k=-\infty}^{+\infty} \mathbf{y}_{(k)} \exp(ik\varphi). \tag{7}$$

After separation of variables, system (4) is decomposed into the infinite amount of linear 8-th order systems of ordinary differential equations (ODE). Each of these ODE systems can be written in matrix notation as follows

$$\frac{d}{ds}\mathbf{y}_{(k)} = \mathbf{F}_{(k)}\mathbf{y}_{(k)} + \mathbf{g}_{(k)} \tag{8}$$

where $\mathbf{F}_{(k)}$ is (8×8) constant square matrix:

$$\mathbf{F}_{(k)} = \begin{bmatrix} 0 & -\frac{i\nu k}{R} & -\frac{\nu}{R} & 0 & \frac{1-\nu^2}{EhR} & 0 & 0 & 0 \\ -\frac{ik}{R} & 0 & 0 & 0 & 0 & \frac{2(1+\nu)}{EhR} & 0 & 0 \\ 0 & 0 & 0 & -1 & 0 & 0 & 0 & 0 \\ 0 & -\frac{i\nu k}{R^2} & -\frac{\nu k^2}{R^2} & 0 & 0 & 0 & 0 & \frac{12(1-\nu^2)}{Eh^3R} \\ \frac{A}{R^2} & 0 & 0 & -\frac{A}{R} & 0 & -\frac{ik}{R} & 0 & 0 \\ 0 & \frac{Ehk^2}{R} & -B & 0 & -\frac{i\nu k}{R} & 0 & 0 & -\frac{i\nu k}{R^2} \\ 0 & B & C & 0 & \frac{\nu}{R} & 0 & 0 & \frac{\nu k^2}{R^2} \\ -\frac{A}{R} & 0 & 0 & A & 0 & 0 & 1 & 0 \end{bmatrix} \tag{9}$$

where E is the Young modulus, ν is the Poisson's ratio, h is the shell's wall-thickness and

$$A = \frac{Eh^3k^2}{6R(1+\nu)},\ B = \frac{iEhk}{R}\left(1+\frac{h^2k^2}{12R^2}\right),\ C = \frac{Eh}{R}\left(1+\frac{h^2k^4}{12R^2}\right). \tag{10}$$

Keeping in mind that $\dim \delta(x) = 1/\dim(x)$, it is quite obvious that

$$\{q_1, q_2, q_3\} = \{0, F_C, -F_R\}\frac{\delta(\varphi)\delta(s-s_F)}{R}. \tag{11}$$

Using the Fourier series of the Dirac delta function

$$\delta(\varphi) = (2\pi)^{-1}\sum_{k=-\infty}^{+\infty}\exp(ik\varphi), \tag{12}$$

the load vector can be rewritten as

$$\mathbf{g}_{(k)} = \frac{1}{2\pi}\{0,\ 0,\ 0,\ 0,\ 0,\ -F_C,\ F_R,\ 0\}\,\delta(s-s_F). \tag{13}$$

The left end of the shell ($s = 0$) is rigidly fixed, and the right end ($s = L$) is free. The followings are the boundary conditions:

$$\begin{aligned} &\{u,\ v,\ w,\ \vartheta_1\}_{(k)} = 0 && \text{at } s = 0 \\ &\{RT_1,\ RS_1^*,\ RQ_1^*,\ RM_1\}_{(k)} = 0 && \text{at } s = L \end{aligned} \tag{14}$$

Here are the continuity conditions at point ($s = s_F$):

$$\mathbf{y}_{(k)}(s_F+\varepsilon) = \mathbf{y}_{(k)}(s_F-\varepsilon) + \frac{1}{2\pi}\{0,\ 0,\ 0,\ 0,\ 0, -F_C,\ F_R,\ 0\} \tag{15}$$

where ε is an infinitesimally small parameter. System (8) along with boundary conditions (14) represent a boundary value problem. We have used the initial pa-

rameters method [6] in order to solve this problem by means of numerical integration. The Godunov orthogonalization method [7] was incorporated to ensure numerical stability of the solution. Moreover, the method was further modified in order to eliminate the well-known Gram-Schmidt process's weakness [8]. The Gram-Schmidt process was replaced by the Householder transformation [9], which effectively performs the same thing—orthonormalizes a set of vectors in the Euclidean space $\mathbb{R}^n$. Harmonic $w_{(k)}(L)$ that corresponds to the radial displacements of points located on the free end of the shell, can be represented as a linear combination of the cutting force components:

$$w_{(k)}(L) = F_C \cdot \alpha_{(k)} + F_R \cdot \beta_{(k)} \tag{16}$$

where coefficients $\alpha_{(k)}$ and $\beta_{(k)}$ depend only on parameter Λ and have been obtained after numerical integration of the boundary value problem for different harmonics. According to expression (7),

$$w_{(k)}(L, \varphi) = \sum_{k=-\infty}^{+\infty} \left(F_C \alpha_{(k)} + F_R \beta_{(k)}\right) \exp(ik\varphi) \tag{17}$$

According to the definition (see Fig. 1), we can write that $w_A = w(L, \Phi_1)$ and $w_B = w(L, \Phi_2)$. Finally, according to formulas (1) and (2), matrix $\mathbf{A}$ can be represented as an infinite series

$$\mathbf{A} = \sum_{k=-\infty}^{+\infty} \begin{bmatrix} \alpha_{(k)} \exp(ik\Phi_1) & \beta_{(k)} \exp(ik\Phi_1) \\ \alpha_{(k)} \exp(-ik\Phi_2) & \beta_{(k)} \exp(-ik\Phi_2) \end{bmatrix}. \tag{18}$$

It can be shown that the components of matrix $\mathbf{A}$ are always real numbers, which they must be, of course, since $\mathbf{A}$ is the flexibility matrix. The criteria of meeting the required accuracy has been

$$\|\mathbf{A}_{N+5} - \mathbf{A}_N\| \cdot \|\mathbf{A}_N\|^{-1} \leq \varepsilon. \tag{19}$$

If the above inequality is satisfied, then we consider approximation $\mathbf{A}_N$ to be accurate enough. In our work, we have set the relative accuracy to $\varepsilon = 0.01 = 1\%$.

The magnitude of the cutting force is approximately 10^2–10^3 N, according to [4]. Using this data and our model, we have calculated that magnitudes of the displacements are within 10^{-5} m.

The components of matrix $\mathbf{A}$ are dependent on the three variable parameters that we have introduced earlier: $\mathbf{A} = \mathbf{A}(\Phi_1, \Phi_2, \Lambda)$.

3.0 Optimization of the Displacement Sensors Location

We need to determine the best set of parameters Φ_1 and Φ_2 (the displacement sensors angular location) that would make the system (1) as well-conditioned as possible. Measure of a square matrix's numerical stability is called its condition number μ. By definition [8],

$$\mu(\mathbf{A}) = \|\mathbf{A}\| \cdot \|\mathbf{A}^{-1}\| . \tag{20}$$

Condition number μ is always positive and cannot be less than one. The closer the condition number μ of the flexibility matrix $\mathbf{A}$ is to one, the better conditioned this matrix is. Therefore, to ensure the best numerical stability of the linear transformation (1) we must minimize the condition number μ of matrix $\mathbf{A}$. Let us construct the target function

$$f(\Phi_1, \Phi_2) = \max_{\Lambda}\left[\mu\left(\mathbf{A}(\Phi_1, \Phi_2, \Lambda)\right)\right] . \tag{21}$$

To accomplish our optimization goal we have had to minimize f:

$$f \to \min, \qquad \left\{\Phi_1^{\text{opt}}, \Phi_2^{\text{opt}}\right\} = \arg\left[\min_{\Phi_1 \in [0,2\pi] \& \Phi_2 \in [0,\pi]} f(\Phi_1, \Phi_2)\right]. \tag{22}$$

We have implemented the brute force approach minimizing function f. Angular increment has been set to $0.1°$, and the increment for parameter Λ has been set to 0.05. Color plot of function $\mu^{-1}\left(\mathbf{A}(\Phi_1, \Phi_2, 1)\right)$ is shown in Fig. 4. We have chosen to analyze function inverse to the condition number because this function is normalized: its range of values lies inside interval $(0, 1)$. The diagram reveals 20 *local maxima* of f (see Fig. 4 and Table 1). The best choice of parameters (i.e. the *global maxima*) turned out to be $\Phi_1^{\text{opt}} = \Phi_2^{\text{opt}} = 20.4°$, which corresponds to the target function value of 1.2. This displacement sensors' configuration is shown in Fig. 3.

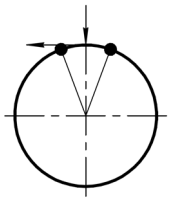

Fig. 3 Optimal displacement sensors location.

Strictly speaking, this value is the global minimum of function $f(\Phi_1, \Phi_2)$. However, in practical terms, any of the displacement sensors configurations from Table 1 can be chosen because magnitude of f for any of those configurations does not even exceed the value of 10. It means that at the worst case scenario we could lose 1–2 significant digits [8] calculating the components of the cutting force using

equation (1), which corresponds to relative accuracy $\varepsilon = 10^{-10}$. Such loss is not significant in comparison with other sources of error in our model.

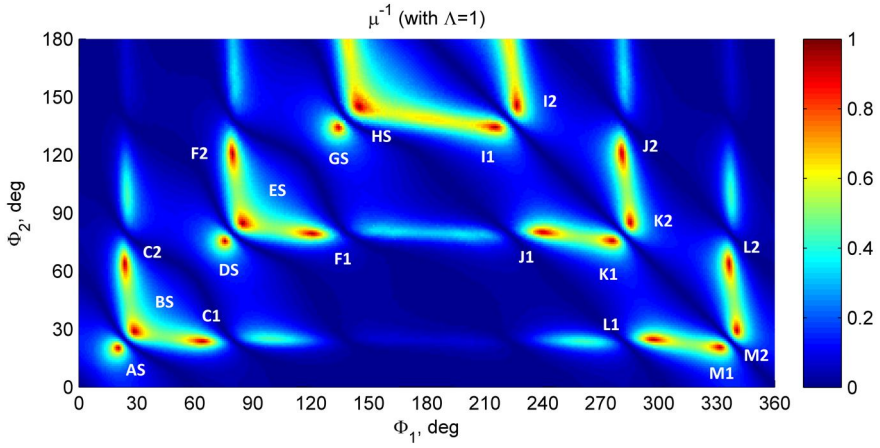

Fig. 4 Optimal displacement sensors' angular location configurations.

Table. 1 Optimal displacement sensors angular location configurations.

#	Φ_1	Φ_2	f	$\|\|\mathbf{A}\|\| \cdot 10^6$	#	Φ_1	Φ_2	f	$\|\|\mathbf{A}\|\| \cdot 10^6$
AS	20.4°	20.4°	1.2	8.2	I1	208.3°	137.5°	1.8	0.59
BS	30.6°	30.6°	1.5	7.2	I2	222.5°	151.7°	1.8	0.59
C1	66.6°	24.3°	1.5	9.7	J1	241.1°	83.5°	2.0	2.1
C2	24.3°	66.6°	1.5	9.7	J2	276.5°	119.9°	2.0	2.1
DS	77.7°	77.7°	2.8	3.8	K1	268.5°	78.6°	2.0	2.7
ES	89.3°	89.3°	1.9	1.6	K2	281.5°	91.5°	2.0	2.7
F1	119.4°	83.5°	1.4	2.2	L1	293.5°	25.3°	1.4	7.1
F2	83.5°	119.4°	1.4	2.2	L2	334.7°	66.5°	1.4	7.1
GS	136.2°	136.2°	1.4	0.87	M1	329.3°	20.5°	1.2	7.6
HS	149.5°	149.5°	1.7	0.37	M2	339.5°	30.7°	1.2	7.6

Index 'S' in Table 1 represents y-symmetrical configurations, and indexes '1' and '2' represent identical configurations. Table 1 also features minimum value of norm of matrix **A,** which represents magnitude of displacements of measured points. Note that

$$\dim \mathbf{A} = \dim \|\mathbf{A}\| = \mathrm{mm/N}. \tag{23}$$

We can see that configurations GS, HS, I1 and I2 are probably not preferable because the displacements would be significantly smaller than in the other configurations. From this point of view, configurations AS, BS, C1, C2, L1, L2, M1, M2 are optimal, and each of them can be readily picked by an experimenter.

4.0 Conclusion

In this work we have developed a mathematical model in order to be able to calculate the flexibility matrix that makes it possible to estimate the cutting force components based on displacement measurement in turning cylindrical shells. Analysis of the behavior of the flexibility matrix condition number has been performed. Based on this analysis, optimal configurations of the displacement sensors location have been suggested. These configurations make the flexibility matrix well-conditioned and the process of calculating the components of the cutting force numerically stable. Any of these configurations can be picked as they do not cause numerical instabilities when calculating the flexibility matrix.

References

[1] Fang N., Q. Wu. A Comparative Study of the Cutting Forces in High Speed Machining of Ti-6Al-4V and Inconel 718 with a Round Cutting Edge Tool. Journal of Materials Processing Technology. 2009. Vol. 209 (9). Pp. 4385–4389.

[2] Sun S., Brandt M., Dargusch M.S. Characteristics of cutting forces and chip formation in machining of titanium alloys. International Journal of Machine Tools and Manufacture. Vol. 49 (7–8). Pp. 561–568.

[3] Kim Tae-Yong, Kim Jongwon. Adaptive cutting force control for a machining center by using indirect cutting force measurements. International Journal of Machine Tools and Manufacture. Vol. 36 (8). Pp. 925–937.

[4] Lorong P., Larue A., and Duarte A. P. Dynamic Study of Thin Wall Part Turning. Advanced Materials Research. 2011. Vol. 223. Pp. 591–599. DOI: 10.4028.

[5] Gerasimenko A. A., Gouskov A. M., Guskov M. A., Lorong P. Spinning shell eigen modes calculation. Vestnik MGTU imeni Baumana, 2012.

[6] Biderman, V. L. Mekhanika tonkostennykh konstruktsiy. Moscow, 1997.

[7] Godunov, S. K. 1961 On the numerical solution of boundary value problems for systems of linear ordinary differential equations. Uspehi. Mat. Nauk. 16, 171–174.

[8] Higham N. J. Accuracy and Stability of Numerical Algorithms. 2nd ed. Philadelphia: SIAM. 2002.

[9] Householder A. S. Unitary Triangularization of a Nonsymmetric Matrix. Journal of the ACM. 1958. Vol. 5 (4). Pp. 339–342. DOI:10.1145/320941.320947.

[10] Kondratenko K. E., Gouskov A. M., Guskov M. A., Lorong. P., Panovko G. Ya. Analysis of indirect measurement of cutting forces in turning metal cylindrical shells. Vestnik MGTU imeni Baumana, 2014. DOI: 10.7463/0214.0687971.